

MASSACHUSETTS INSTITUTE OF TECHNOLOGY
ARTIFICIAL INTELLIGENCE LABORATORY

A.I. Memo No. 1331

December, 1994

Dynamic Model and Control of an Artificial Muscle based on Contractile Polymers

David L. Brock

Abstract: A dynamic model and control system of an artificial muscle is presented. The artificial muscle is based on a contractile polymer gel which undergoes abrupt volume changes in response to variations in external conditions. The device uses an acid-base reaction to directly convert chemical to mechanical energy. A nonlinear sliding mode control system is proposed to track desired joint trajectories of a single link controlled by two antagonist muscles. Both the model and controller were implemented and produced acceptable tracking performance at 2Hz.

This report describes research done at the Artificial Intelligence Laboratory of the Massachusetts Institute of Technology. Support for this research has been provided the Defense Advanced Research Projects Agency under contract number N00014-91-J-1698.

©Massachusetts Institute of Technology, 1991

1 Introduction

In 1950 W. Kuhn and A. Katchalsky produced a fiber which contracts in response to changes in pH (Kuhn 1950). In their demonstration a single fiber immersed in a fluid repeatedly raised and lowered a weight proportional to the hydrogen ion content of the solvent. It was proposed at the time that such a device could be used as a linear actuator. One of the major drawbacks however was the exceedingly slow response time, on the order of minutes. Since then a number of innovations have made this artificial “muscle” worthy of further study. First, fibers have been produced which contract in seconds and even tenths of seconds (DeRossi 1987; Suzuki 1989). Second, some fibers support considerable loads, on the order of $100\text{N}/\text{cm}^2$ (DeRossi 1988). The contraction rates and forces have become comparable, and in some cases even exceeding, that of a human muscle. Third, the physics of fiber contraction (or gels as they are more generally called) have become well understood (Tanaka 1973a - 87b). Finally, technological innovations such as robotics and implantable artificial biological organs have created a demand for such devices. A number of contractile gel devices have already been constructed, such as a robot gripper (Caldwell 1990), a multifingered hand (Toyota 1990), and an artificial urethral sphincter (Chiarelli 1988; DeRossi 1985; 86).

The design of these devices from a practical engineering perspective, particularly with regard to dynamic modeling and control has only been considered recently (Genuini 1990).

In this paper we will consider the design of a simple linear actuator based on contractile gel fibers as well as the design and simulation of single mechanical linkage controlled by two antagonist muscles. The first section will discuss the design of a simple linear actuator and the second will present a dynamic model along with approximate parameter estimates. The third section will introduce a nonlinear sliding mode controller which achieves desired trajectory tracking for model inputs.

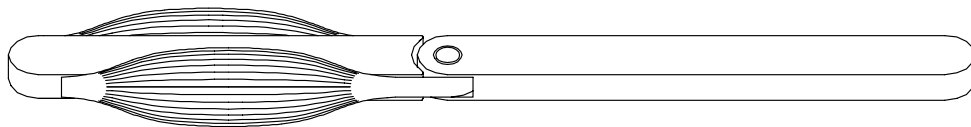


Figure 1-1. Two antagonist artificial muscles control a single link.

2 Design

Although there are many possible actuator designs, this paper will focus on the direct chemical to mechanical energy conversion through the control of the hydro-

gen ion content in the muscle fibers. The basic concept is to use high performance miniature valves to control the inflow of acid or base to modulate pH and control contraction. A schematic diagram of the proposed actuator is shown in figure 2-1. Two input lines containing 0.1M HCL and 0.1M NaOH enter the muscle at the base. A miniature valve placed into the base material controls the inflow of fluid. An irrigation system design to facilitate mixing is composed of numerous small tubes which are interspersed among the fibers. Finally, a drainage tube allows the waste fluid (i.e. salt water) to be removed.

The tubes and wetting surfaces of the valves are constructed from teflon which is chemically inert and the fibers are made from Poly-Vinyl Alcohol PVA. Although many different contractile materials exist (Tanaka 1990), PVA has been used successfully by a number of researchers and has a relatively high tensile strength. The tendons are made of Spectra and the tendon to PVA connections are machined Delran. The fibers are affixed at their terminations with epoxy which is also chemically inert.

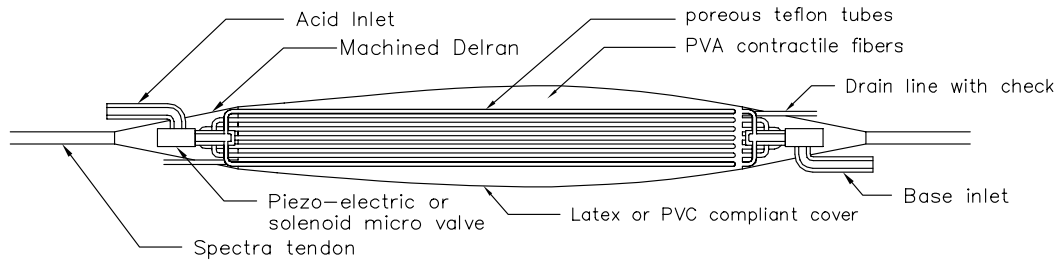


Figure 2-1. Two fluid microvalves meter desired amounts of acid or base through an irrigation system to a bundle of contractile fibers.

3 Model

The dynamic model of the system is composed of three basic parts: the fluid conveyance system, the hydrogel contractile fibers and the mechanical linkage. The following sections will address each of these systems in detail.

3.1 Fluid System

A schematic diagram of the fluid system is shown in figure 3-1. It is assumed the inlet fluid line is under a moderate pressure P_o and a microvalve with controllable resistance R_v modulates the inflow of fluid. The system of irrigation lines is modeled as a fluid resistance R_T and an inertance I . Finally, the compliant sheath into which the fluid flows is modeled as a capacitance C and the exit line, a resistance R_e .

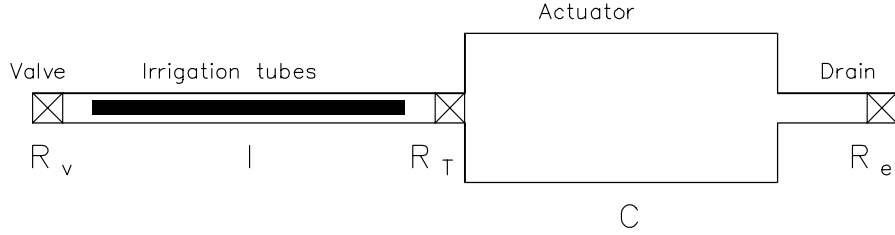


Figure 3-1. The fluid model consists of a pressure source P_o at the inlet of the system. The valve, tubes and drain line are modeled as fluid resistances R_v , R_T and R_e respectively. Finally, a fluid inertia I is included to account for the mass of the fluid and a capacitance C to model the expansion of the actuator chamber.

Valve

Although there are commercially available metering valves which continuously modulate flow, they are generally too large from this application. Commercial piezo-electric or solenoid fluid valves also exist in the appropriate size, although they have only two states, open and closed. It may be possible to use binary state valves in a pulse width modulation scheme to meter fluid, but this may introduce undesirable affects such as water hammer, excessive part wear and slower response. Alternatively there are some experimental metering valves and pumps which are of the correct dimension (in fact some are significantly smaller than this application demands creating the possibility of very small linear actuators). It may also be possible to use molecular valves in the form of biological or artificial membranes whose porosity is controlled by small voltages.

In any case it is assume some mechanical valve of the appropriate dimension can be constructed, either a commercial two-state valve or an experimental multi-state valve. Based on commercial data sheets for fluid resistance we can approximate the resistance of a valve by

$$R_v = a(bu_v)^n,$$

where R_v is fluid resistance in $N^{1/2}sm^{-4}$, $a = 4.09 \times 10^3 N^{1/2}sm^{-4}$, $b = 2.5 \times 10^{-4} m/v$, and $n = -1.7925$ are constants. For two-state valves we will assume $u_v = u_o + \text{sgn}(u)$ and for multi-state valves $u_v = u_o + u$, where u_o is some small value and u is the control signal input, 0 to 12 v. These parameters were roughly based on values given for the LEE Interface Fluidic 2-way (normally closed) microvalve. This valve is energized with 12 v at 250mW, switches in 1.5 msec and operates in a 0 to 7 psi pressure range. The relation of pressure to flow is given by

$$R_v^2 Q_v^2 = P_v,$$

where Q_v is flow rate in m^3/s , P_v is pressure in N/m^2 and R_v is fluid resistance $N^{1/2}sm^{-4}$.

Irrigation System

Multiple porous tubes attempt to uniformly enter and mix the fluid to increase the response time of the actuator. Consider a single tube as shown in figure 3-2. The tube has an inner radius $r = 0.76$ mm and a straight length $l = 10$ cm after a 90° elbow of radius $r_e = 4r = 0.30$ cm. Small holes of radius 0.1 mm are punctured in the teflon tubes. The holes are small enough so that an initial pressure P_m is necessary to induce flow. This prevents back flow into the acid-base lines, but for this initial model we will assume P_m is zero. The holes are placed at 90° intervals about the cross section and every 1 mm along the length.

Suppose the tube as we describe is non-porous and open at the end. If we assume a fully developed flow under an entrance pressure of $P_o = 1$ kPa (above atmospheric), the fluid flow is

$$Q = \frac{\pi P_o r^4}{8\mu l}, \quad (1)$$

where $\mu = \rho\nu = 10^{-3}$ kg/m s (for water, 25°C), $r = 7.60 \times 10^{-4}$ m, and $l = 0.1$ m. This yields a flow of $Q = 1.3 \times 10^{-6}$ m³/s and an average fluid velocity of $u_{avg} = Q/\pi r^2 = 0.72$ m/s. The Reynolds number is $\text{Re} = vd/\nu = 1089$, where $v = u_{avg}$, $d = 1.52 \times 10^{-3}$ m and $\nu = 10^{-6}$ m²/s, which is below the critical value $\text{Re}_{d,crit} = 2300$; therefore we may assume the flow is laminar. For higher pressures, equation 1 yields Reynolds numbers in the turbulent range, but the significant resistance offered by the sealed porous tube reduce the flow rates and maintains laminar conditions. As we will later show the maximum flow rate is approximately $Q_{max} = 1.65 \times 10^{-7}$ m³/s, which yields $u_{avg} = 0.1$ m/s and $\text{Re} = 152$, which is certainly laminar. Finally, the entrance region before the fully developed flow is approximately $l_e = 0.06 \text{ Re } d = 1.4$ cm; therefore we can assume the boundary layer is fully develop within the entire length of the tube.

The wall shear force will result in a head loss and thereby create non-uniformity flows through the small irrigation holes. However, since the flow will decrease along the length due to seepage, the head loss will not be linear as in the case of homogeneous circular tubes. To approximate the head loss we will assume continuous porosity and a uniform fully developed flow at each point x of tube. The wall shear stress is given by

$$\tau_w(x) = \frac{4\mu Q(x)}{\pi r^3},$$

which results in a pressure gradient

$$\frac{dP(x)}{dx} = \frac{-8\mu Q(x)}{\pi r^4}.$$

If we assume a flow loss due to porosity

$$\frac{dQ(x)}{dx} = -aP(x),$$

we have the resulting differential equation

$$\frac{dP(x)^2}{d^2x} = bP(x),$$

where $b = 8a\mu/\pi r^4$. If we solve this differential equation with boundary conditions $P(0) = P_o$ and $Q(l) = 0$, we have the head loss as a function of length

$$P(x) = \frac{P_o}{1 + e^{2cl}}(e^{cx} + e^{2cl}e^{-cx}),$$

where $c = \sqrt{b} = 3.4 \text{ m}^{-1}$. The head loss in the tube is not significant in this case as shown in figure 3-2.

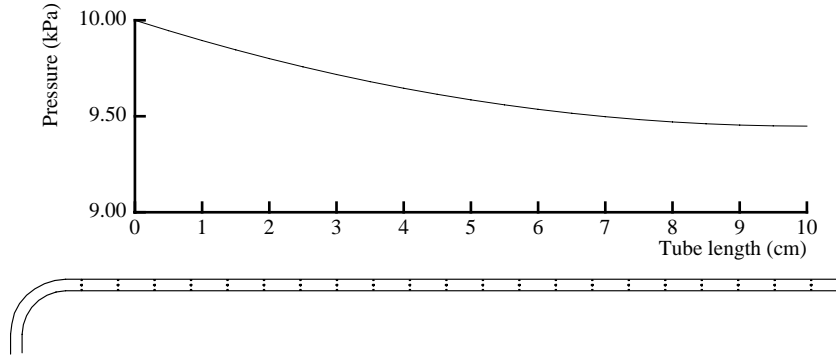


Figure 3-2. Head loss due to wall shear force in the circular porous tube can generally be ignored.

For the purposes of the dynamic model, it may be more more useful to represent the entire porous tube system as a fluid resistance R_T . Following a simplified convention, we will assume the fluid resistance is given by

$$R = R_o + \rho l,$$

where R is fluid resistance R_o is the resistance due to the entrance, ρ is the resistance per unit length and l is the length of the tube. The entrance resistance is given by

$$R_o = ad^n, \tag{2}$$

where d is the inner diameter of the tube in meters, $a = 4.1 \times 10^3$ and $n = -1.8$. For the tubes 0.152 cm in diameter $R_o = 4.6 \times 10^8 \text{ N}^{1/2}\text{sm}^{-4}$. The resistance per unit length

$$\rho = a_\rho d^{n_\rho},$$

where $a_\rho = 1.22 \times 10^6 \text{ N}^{1/2}\text{sm}^{-4}$, $n_\rho = -2$, and d is the inner diameter. For the tube described above, the resistance per unit length is $\rho = 5.3 \times 10^8 \text{ N}^{1/2}\text{sm}^{-5}$, thus the total resistance for the tube is $5.13 \times 10^8 \text{ N}^{1/2}\text{sm}^{-4}$. Using equation ?? to compute the resistance of the irrigation holes, we have a resistance $4.0 \times 10^{10} \text{ N}^{1/2}\text{sm}^{-4}$ for holes 0.1 mm in diameter. However with 80 holes/cm and 10 cm of tube, the total resistance is $1.6 \times 10^8 \text{ N}^{1/2}\text{sm}^{-4}$.

For the acid and base systems we will have six irrigation tubes each, resulting in a total fluid resistance of $R_T = 9.65 \times 10^7 \text{ N}^{1/2}\text{sm}^{-4}$. The relation between pressure and flow is again given by,

$$R_T^2 Q_T^2 = P_T.$$

Inertance

Although the inertance of the fluid is small, fast switching times may cause its effects to be important. The inertance is given by

$$I = \frac{\rho l}{A},$$

where $\rho = 10^3 \text{ kg/m}^3$ is the fluid density, $l = 0.1 \text{ m}$ is the length of the tubes and $A = 1.1 \times 10^{-5} \text{ m}^2$ is the total cross sectional area. For this system, the fluid inertance is $I = 9.2 \times 10^6 \text{ kg/m}^4$ and the dynamics are given by

$$I \dot{Q}_I = P_I.$$

Suppose the fluid accelerates to $1.3 \times 10^{-6} \text{ m}^3/\text{s}$ in 10 ms under a pressure of 1 kPa. Then the inertance I would be $7.7 \times 10^6 \text{ kg/m}^4$. This is comparable to the value given for the model. So for switching times on the order of 1 ms, inertance effects become significant.

Capacitance

In this particular design, the fiber system is covered with a compliant sheath. Since it is flexible, it can be approximated as a fluid capacitance; that is, when fluid is forced into the chamber the sheath will stretch and resist the flow. If we model the sheath as a thin-walled uniform cylinder with closed ends, the elemental stress tensor is given

by $\sigma_r = 0$, $\sigma_\theta = Pr/t$, $\sigma_z = Pr/2t$ and $\tau_{ij} = 0$, where P is the pressure, t is the wall thickness and r is the radius. Given the generalized stress-strain relations,

$$\begin{aligned}\epsilon_r &= \frac{\nu}{E}(\sigma_\theta + \sigma_z) \\ \epsilon_\theta &= \frac{1}{E}(\sigma_\theta - \nu\sigma_z) \\ \epsilon_z &= \frac{1}{E}(\sigma_z - \nu\sigma_\theta),\end{aligned}$$

and the strain-displacement equations

$$\begin{aligned}\Delta r &= r\epsilon_\theta \\ \Delta l &= l\epsilon_z,\end{aligned}$$

we can solve for the change in volume as a function of pressure

$$\Delta V = \left(\frac{\pi r^3 l (3 - 4\nu)}{2Et} \right) P,$$

where E is the Elastic Modulus and ν is Poisson's ratio. Therefore the fluid capacitance is

$$C = \frac{\pi r^3 l (3 - 4\nu)}{2Et}.$$

If $r = 1$ cm, $l = 10$ cm, $E = 10^6$ N/m² (approximate for rubber), $\nu = 0.5$ and $t = 0.1$ mm,

$$C = 1.6 \times 10^{-15} \text{ m}^5/\text{N}.$$

With a fluid flow of $Q = 1.3 \times 10^{-6}$ m³/s, this capacitance will become significant if the pressure changes more than 1 MPa in a 1 ms. Therefore we will ignore the capacitance.

Drain

The drain line consists of a single tube $d_e = 0.3$ cm and a check valve. Employing equation ??, this results in a fluid resistance of $R_e = 2.22 \times 10^8$ N^{1/2}sm⁻⁴, for a drain line 20 cm in length.

Fluid dynamic equations

The elemental pressures are related by

$$P_o = P_v + P_I + P_T + P_e$$

and the flows by

$$Q = Q_v = Q_I = Q_T = Q_e.$$

Substituting the elemental relations, we have

$$\dot{Q} = \frac{1}{I} [P_o - (R_v^2 + R_T^2 + R_e^2)Q^2]$$

where Q is the flow into the fibers. Note the steady state flow rate for the open valve is

$$Q_{ss} = \sqrt{\frac{P_o}{R_v^2 + R_T^2 + R_e^2}}.$$

For a fully open valve $Q_{ss} = 1.65 \times 10^{-7} \text{ m}^3/\text{s}$. Note the total volume of injected fluid is

$$\dot{V} = Q.$$

Mixing and Diffusion

When the fluid (either acid or base) is injected into the fiber network there is a certain lag time before the entire system uniformly equilibrates to the new concentration. We could model this mixing as the diffusion of HCl or NaOH in water. If the tubes are uniformly spaced as in figure 3-3, we can draw concentric circles around each with radius r_o equal to half the distance between the tubes. The mixing time could be approximated, as the time for the fibers at radius r_o to experience a certain concentration of fluid. As a simplification we can approximate the diffusion with the one dimension diffusion equations

$$\begin{aligned} J &= -D \frac{\partial c}{\partial r} \\ \frac{\partial c}{\partial t} &= \frac{\partial^2 c}{\partial r^2}, \end{aligned}$$

where J is the diffusion flux per unit area, c is the concentration in moles per volume and D is a constant. The solution is the standard diffusion model

$$c = c_o \left[1 - \operatorname{erf} \left(\frac{r}{2\sqrt{Dt}} \right) \right],$$

where

$$\text{erf}(x) = \frac{2}{\sqrt{\pi}} \int_0^x e^{-y^2} dy.$$

The boundary concentration c_o , of course, decreases as particles diffuse into the liquid. However, as a first order approximation to the diffusion time, we assume c_o is constant. Then the concentration at r_o is one-half its initial value when $t = 1.4$ ms for $D = 3.05 \times 10^{-4}$ m²/s (0.1M HCL at 25°C) and $r_o = 1.5 \times 10^{-3}$ m.

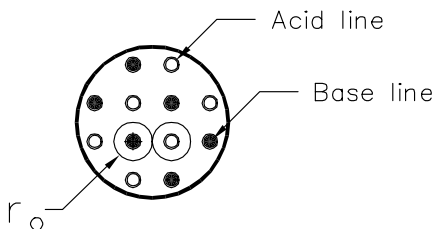


Figure 3-3. Arrangement of acid and base lines in the cross section of the muscle.

The diffusion model, however, is highly inaccurate since the exit velocity from the pores in the teflon tubes is relatively high and together with the motion of the fibers will cause turbulent mixing, not diffusion. Therefore as a simple approximation, we will assume the fluid mixing and diffusion is a first order lag, hence

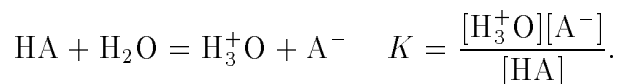
$$\tau_m \dot{c} + c = c_o, \quad (3)$$

where c is the concentration of acid or base in the solvent, τ_m is a time constant which we will take to be $\tau_m = 1.4$ ms (based roughly on the previous discussion) and $c_o = V_i/V_T$ ratio of solute to solvent, where V_T is the total volume of the actuator, $V_T = 2.92 \times 10^{-5}$ m³.

3.2 Contractile Fibers

pH

The contractile fibers respond roughly linearly to pH, so it is important to calculate the pH in the solution based on the amount of acid or base entered into the chamber. An acid is a chemical species having the tendency to lose a proton and a base is a species tending to accept a proton. The quantitative measure of acid strength is the acid dissociation constant; that is the equilibrium constant for the reaction



Along with this reaction there is always the self dissociation of water

$$[\text{H}_3^+\text{O}][\text{OH}^-] = K_w.$$

If the original amount of acid A added to the solution is $[\text{HA}]_o$, then the material balance relation is given by

$$[\text{HA}]_o = [\text{HA}] + [\text{A}^-].$$

Also the solution must be electrically neutral, hence

$$[\text{H}_3^+\text{O}] = [\text{A}^-] + [\text{OH}^-].$$

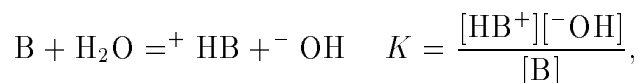
Solving these equations for the hydrogen ion concentration yields the cubic

$$\frac{[\text{H}_3^+\text{O}]([\text{H}_3^+\text{O}] - K_w/[\text{H}_3^+\text{O}])}{[\text{HA}]_o - [\text{H}_3^+\text{O}] + K_w/[\text{H}_3^+\text{O}]} = K$$

However, we may assume that the H_3^+O from water is negligible compared to that from the acid, hence $[\text{H}_3^+\text{O}] = [\text{A}^-]$. We may assume that for strong acids there is complete dissociation; that is $[\text{A}^-] = [\text{HA}]_o$, which yields the trivial result

$$[\text{HA}]_o = [\text{H}_3^+\text{O}].$$

Similarly, for base a B we have equilibrium



mass balance,

$$[\text{B}]_o = [\text{B}] + [^+\text{BH}]$$

and electric neutrality

$$[\text{BH}^+] + [\text{H}_3^+\text{O}] = [^-\text{OH}].$$

Now we can assume total dissociation

$$[\text{B}]_o = [^+\text{BH}],$$

which is a valid except for very high concentrations. Also we can assume the contribution of ^-OH from self-ionization of water is negligible, hence

$$[\text{H}_3^+\text{O}] = \frac{K_w}{[^-\text{OH}]} = \frac{K_w}{[\text{B}]_o}.$$

Considering the strong acid and base together we can assume

$$[\text{H}_3^+\text{O}] = \begin{cases} [\text{HA}]_o - [\text{B}]_o & [\text{HA}]_o - [\text{B}]_o > 0 \\ K_w/([\text{B}]_o - [\text{HA}]) & \text{otherwise} \end{cases} .$$

Since pH is $\text{pH} = -\log[\text{H}_3^+\text{O}]$, we have

$$\text{pH} = \begin{cases} -\log([\text{HA}]_o - [\text{B}]_o) & [\text{HA}]_o - [\text{B}]_o > 0 \\ 14 + \log([\text{B}]_o - [\text{HA}]) & \text{otherwise} \end{cases} .$$

Diffusion

Besides the lag due to mixing among the fibers, there is a lag due to the diffusion within the fibers themselves. This lag is due to bulk macromolecular rearrangement of the polymers in the network and is approximately proportional to the square of the cross sectional diameter. The time constant is

$$\tau = cd^2,$$

where d is the diameter in meters and $c = 2 \times 10^9 \text{ s/m}^2$. Thus for fibers 10 μm in diameter contract in approximately 0.1 s. This can also be approximated to the first order by

$$\tau \dot{\text{pH}} + \text{pH} = \text{pH}_s,$$

where $\tau = 0.2$, pH is the pH in the fiber and pH_s is that in the solvent. Notice this time constant is substantially slower than the one given in equation ???. Therefore we will ignore the lag due to mixing and consider only the diffusion within the fiber as the major delay.

Hydrogel Physics

A gel is a cross-linked network of polymers immersed in a fluid, which can undergo a volume phase transition in response to changes in external conditions such as temperature, solvent, pH, light and electric fields. Three competing forces act on the polymer gel network: rubber elasticity, polymer-polymer affinity and hydrogen ion pressure. Competition between these forces, collectively called the *osmotic pressure*, determine the equilibrium volume of the network. The phase transition has been analyzed in terms of the mean field theory of swelling equilibrium of gels. The osmotic pressure of a gel is given by Flory's equation,

$$\pi = -\frac{NkT}{v_1} \left[\phi + \ln(1 - \phi) + \frac{\Delta F}{2kT} \phi^2 \right] + \nu kT \left[\frac{\phi}{2\phi_o} - \left(\frac{\phi}{\phi_o} \right)^{1/3} \right] + \nu f kT \left(\frac{\phi}{\phi_o} \right),$$

where N is Avogadro's number, k is the Boltzmann constant, $\Delta F = \Delta H - T\Delta S$ represents the difference between the free energies of a polymer segment-segment and polymer-solvent interaction, and ΔH and ΔS are the enthalpy and entropy respectively. In equilibrium, the osmotic pressure is zero. Thus by solving the above equation, we can theoretically compute the fiber force. However because of its complexity and because of the availability of empirical data, we can describe the contraction of the fiber with the simple model shown in figure 3-4. The intrinsic force per unit area is f_m is approximately

$$f_m = 1.0 \times 10^5 \text{N/m}^2 (7 - \text{pH}_f),$$

assuming a total cross sectional area $2.92 \times 10^{-4} \text{ m}^2$, the intrinsic force is $F_m = 29.2 \text{ N}(7 - \text{pH}_f)$. Also the intrinsic stiffness is

$$k_m = 1.43 \times 10^3 \text{N/m}.$$

and viscous damping is roughly estimated as

$$b_m = 30 \text{Ns/m}.$$

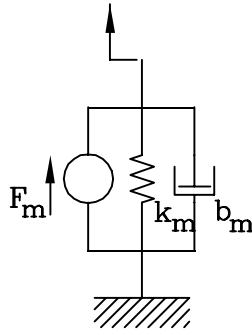


Figure 3-4. Simple model of contractile fiber.

3.3 Mechanical System

A model of the mechanical system is shown in figure 3-5. Assuming linear components for this part of the model, we have

$$J\ddot{\theta} + (B + 2R^2b_m)\dot{\theta} + 2R^2k_m\theta = R(F_1 - F_2),$$

where

J	$1.28 \times 10^{-4} \text{ kg m}^2$	Link inertia
B	neg.	Joint damping
R	1.7 cm	Pulley radius
b_m	0.7 N s/m.	Actuator damping
k_m	$1.43 \times 10^3 \text{ N/m}$	Actuator stiffness
θ	rads	Joint angle
F_i	$29.2 \text{ N}(7 - \text{pH}_i)$	Controllable force for i^{th} actuator

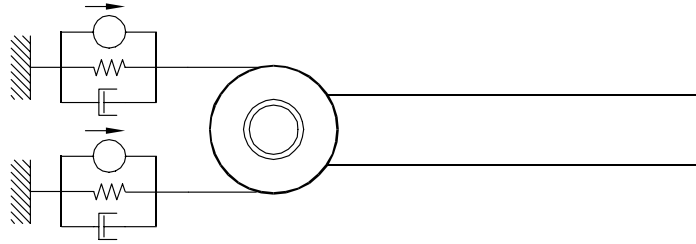


Figure 3-5. Single link controlled by two antagonist muscles.

3.4 Summary

Using the model as outlined above we have the following system equations

$$\begin{aligned}
 \dot{Q}_i &= (P_o - (R_t^2 + R_e^2)Q_i^2 - a^2(b(u_o + |u|))^{2n}Q_i^2)/I \\
 \dot{V}_i &= Q_i \text{sgn}(u) \\
 \dot{\text{pH}}_i &= (-\text{pH}_i - \log(10^{-7} + V_i/V_T))/\tau \\
 \ddot{\theta} &= -(B + 2R^2b_m)\dot{\theta} - 2R^2k_m\theta + R(F_1 - F_2)/J.
 \end{aligned}$$

However before we design a controller for this system let us consider a number of simplifications. First, the lag due to the inertance of the fluid is negligible compared with the dynamics of the rest of the system. This was verified in a full dynamic simulation of the system, although it is fairly obvious since the time constant of the fluid flow is on the order of 10 ms while the diffusion lag is about 100 ms. This assumption allows us to compute the flow Q directly from the input u . Thus we can reduce the order of the system by two and take the input to be the flow rate Q_i . In order to simplify this problem further let us assume a single-input single-output system, by taking the co-contraction of the actuators as an offset force and controlling position through feedback through a single actuator. With these initial assumptions let us write the system equations in the form

$$\dot{\mathbf{x}} = \mathbf{f}(\mathbf{x}, \mathbf{u}).$$

Specifically,

$$\begin{aligned}
 \dot{x}_1 &= u \\
 \dot{x}_2 &= a_1 x_2 + a_1 \log(a_2 + a_3 x_1) \\
 \dot{x}_3 &= x_4 \\
 \dot{x}_4 &= a_4 x_4 + a_5 x_3 + a_6 + a_7 x_2
 \end{aligned}$$

where

$$\begin{aligned}
 x_1 &= V(\text{cm}^3) \\
 x_2 &= pH \\
 x_3 &= \theta \\
 x_4 &= \dot{\theta}
 \end{aligned}$$

and

$$\begin{aligned}
 a_1 &= -33 \text{ s}^{-1} \\
 a_2 &= 10^{-7} \\
 a_3 &= 0.343 \text{ cm}^{-3} \\
 a_4 &= -135 \text{ s}^{-1} \\
 a_5 &= -6457 \text{ s}^{-2} \\
 a_6 &= 2.89 \times 10^4 \text{ s}^{-2} \\
 a_7 &= -3.87 \times 10^3 \text{ s}^{-2}
 \end{aligned}$$

4 Control

We wish to control the joint angle $x_3 = \theta$ using the simplified model presented above. We would also like the controller to maintain zero tracking error in the presence of modeling errors. Therefore, we will design a non-linear sliding mode controller.

However before we attempt to construct a controller for this fourth order system, let us initially consider one further simplification. Based on the numerical estimates of the model parameters the damping ratio of the linear mechanical dynamics is $\zeta = 1.4$. Therefore let us initially assume the inertia can be neglected, and produce a controller based on the reduced third order system,

$$\begin{aligned}
 \dot{x}_1 &= u \\
 \dot{x}_2 &= a_1 x_2 + a_1 \log(a_2 + a_3 x_1) \\
 \dot{x}_3 &= a_4 x_3 + a_5 + a_6 x_2
 \end{aligned}$$

where

$$\begin{aligned}x_1 &= V(\text{cm}^3) \\x_2 &= pH \\x_3 &= \theta\end{aligned}$$

and

$$\begin{aligned}a_1 &= -33 \text{ s}^{-1} \\a_2 &= 10^{-7} \\a_3 &= 0.343 \text{ cm}^{-3} \\a_4 &= -48 \\a_5 &= 201 \\a_6 &= -28.6\end{aligned}$$

Now the *controllability canonical form*,

$$x^{(n)} = f(\mathbf{x}) + b(\mathbf{x})u,$$

where $\mathbf{x} = [x, \dot{x}, \dots, x^{(n-1)}]^T$, can be derived by differentiating the equation for the joint angle three times.

$$\begin{aligned}\ddot{x}_3 &= a_1 a_6 \log(a_2 + a_3 x_1) + (a_1 a_6 + a_4 a_6) x_2 + a_4^2 x_3 + a_5 a_4 \\x_3^{(3)} &= a_1 a_6 (a_1 + a_4) \log(a_2 + a_3 x_1) + (a_1 a_6 (a_1 + a_4) + a_4^2 a_6) x_2 \\&\quad a_4^3 x_3 + a_4 a_5 + \frac{a_1 a_6}{(a_2 + a_3 x_1)} u\end{aligned}$$

Let $\tilde{\mathbf{x}} = \mathbf{x} - \mathbf{x}_d$ be the tracking error on \mathbf{x} and define the *sliding surface* to be $S(t) = \{\mathbf{x} \in \mathfrak{R}^5 | s(x, t) = 0\}$, where

$$s(\mathbf{x}, t) = \left(\frac{d}{dt} + \lambda \right)^{n-1} \tilde{x},$$

for some positive λ . Hence

$$s = \ddot{\tilde{x}} + 2\lambda\dot{\tilde{x}} + \lambda^2\tilde{x}.$$

Thus maintaining zero tracking error is equivalent to the first-order stabilization problem in s . In addition a bound on s implies a bound on the tracking error vector; that is if $|s(t)| \leq \Phi$, then $|\tilde{x}(t)^{(i)}| \leq (2\lambda)^i \epsilon$. We must now design a controller such that for all $\mathbf{x} \notin S(t)$,

$$\frac{1}{2} \frac{d}{dt} s^2(x, t) \leq \eta |s(x, t)|,$$

for some positive η . The estimation of f is given by \hat{f} and the bounds on the error is

$$|f - \hat{f}| \leq F.$$

Similarly, the term b is estimated by $\hat{b} = \sqrt{b_{\min} b_{\max}}$ where $0 < b_{\min} \leq b \leq b_{\max}$. If we let $\beta = \sqrt{b_{\max}/b_{\min}}$, then

$$\frac{1}{\beta} \leq \frac{b}{\hat{b}} \leq \beta.$$

and the control law

$$u = \hat{b}^{-1}(\hat{u} - k \operatorname{sgn}(s))$$

for s given above,

$$k = \beta(F + \nu) + (\beta - 1)|\hat{u}|,$$

and

$$\hat{u} = -\hat{f} + x_d^{(3)} - \lambda \ddot{x} - \lambda^2 \dot{x}.$$

In this case we chose $\lambda = 10 \text{ s}^{-1}$ to be approximately equal to the natural frequency of the system while the estimate errors to be approximately 10% the nominal values.

5 Simulation

In order to get a sense of the model dynamics a 1Hz sinusoidal input was given to the system. A plot of the pH as a function of time is shown in figure 5-1 and the joint angle in figure 5-2. The sliding mode controller discussed in the previous section was implemented and simulated for a desired joint trajectory

$$x_d = \sin(2\pi t) + 1.5.$$

Figure 5-3 shows the pH and figure 5-4 shows the desired and actual joint position. Notice desired tracking is achieved after approximately 0.5 seconds. Figure 5-5 shows the effect of neglected link inertia. Note the joint trajectory is offset by approximately 10° . Fourth and fifth order sliding mode controllers were attempted to compensate for the link inertia and fluid inertance, but were found to be numerically unstable in the calculation of the higher order derivatives. Numerical filters corrected this problem, though the simulation times became unacceptable long. A more judicious choice of numerical parameters could possibly correct this problem.

Figure 5-1. pH in the polymers fibers in response to a 1Hz input signal.

Figure 5-2. Joint angle.

Figure 5-3. Response of pH to control of joint trajectory.

Figure 5-4. Desired and actual (modeled) joint trajectories. Zero tracking error is achieved after one second.

Figure 5-5. Effect of neglected joint inertia.

6 Conclusion

A sliding mode controller produced reasonable tracking performance for input sine waves on the order of 1-2 Hz, but deviated significantly at higher frequencies. This seems reasonable based on the relatively long lag times introduced by the polymer diffusion. It has been possible more recently, to produce even smaller fibers (about 1 μm), while using UV induced transectional cross-linking to increase strength. These and other innovations should allow faster response times for practical actuator development and controller design.

REFERENCES

1. Chiarelli, P. and De Rossi, D., "Determination of Mechanical Parameters related to the Kinetics of Swelling in an Electrically Activated Contractile Gel," *Progress in Colloid and Polymer Science*, Vol. 48, 1988.
2. ———, et. al., "Progress in the Design of an Artificial Urethral Sphincter," *Proc. of the 3rd Vienna International Workshop on Functional Electrostimulation*, Vienna Austria, Sept. 1989.
3. ———, et. al., "Dynamics of a Hydrogel Strip," In Press, *Biorheology*, 1990.
4. ———, Umezawa, K, and De Rossi, D., "A Polymer Composite showing Electrocontractile Response," submitted to *Journal of Polymer Science Polymer Letters Edition*
5. De Rossi, D., et. al., "Electrically Induced Contractile Phenomena in Charged Polymer Networks Preliminary Study on the Feasibility of the Muscle-like Structures," *Transactions of the American Society of Artificial Internal Organs XXXI*, p. 60-65, 1985.
6. ———, et. al., "Contractile Behavior of Electrically Activated Mechanochemical Polymer Actuators," *Transactions of the American Society of Artificial Internal Organs XXXII*, p. 157-162, 1986.
7. ——— and Chiarelli, P., "Determination of Mechanical Parameters related to the Kinetics of Swelling in an Electrochemically Actuated Contractile Gel," *Abstract 5th. International Seminar on Polymer Physics*, High Tatras, 1987.
8. ———, et. al., "Analogues of Biological Tissues for Mechanoelectrical Transduction: Tactile Sensors and Muscle-Like Actuators," *NATO ASI Series*, Vol. F43, Sensors and Sensory Systems, 1988.
9. Genuini, G., et. al., "Pseudomuscular Linear Actuators: Modeling and Simulation Experiences in the Motion of Articulated Chains," In Press, *NATO ASI Science*, 1990.
10. Itoh, Y., et. al., "Contraction/Elongation Mechanism of Acrylonitrile Gel Fibers," *Polymer Preprints - Japan (English Edition)*, Vol. 36, Nos. 5-10, p. E184, 1987.
11. Katchalsky, A., et. al., Chapter "Elementary Mechanochemical Processes," *Size and Shape Changes of Contractile Polymers*, Wassermann, A. ed., Pergamon Press, New York, 1960.
12. ———, et. al., "Reversible Dilatation and Contraction by Changing the State of Ionization of High-polymer Networks," *Nature*, Vol. 165, p. 514-516.

13. ———, Remel, A. and Walters, D. H., "Conversion of Chemical into Mechanical Energy by Homogeneous and Cross-striated Polymeric Systems," in Wassermann, A., (ed.), *Size and Shape Changes of Contractile Polymers*, Pergamon Press, New York, p. 41-77, 1960.
14. Kuhn, W., et. al., "Reversible Dilatation and Contraction by Changing the State of Ionization of High-polymer Acid Networks," *Nature*, Vol. 165, p. 514-516, 1950.
15. ——— and Tanaka, T., "Study of the Universality Class of the Gel Network System," *Journal of Chemical Physics*, Vol. 90, No. 9, p.5161-5166, 1989.
16. Morasso, P., et. al., "Generation of Command Synergies for Anthropomorphic Robots," *Proc. IEEE of the Conference on Robotics and Automation*, 1990.
17. Matsuo, Eriko Sato and Tanaka, Toyochi, "Kinetics of discontinuous volume-phase transition of gels", *Journal of Chemical Physics*, Vol. 89, No. 3, 1988.
18. Nakatani, Y., Ourisson, G. and Tanaka, T., "Osmotic Swelling of Phospholipid Vesicles," *Biophysics Biochemical Research Communications*, Vol. 110, p. 1320, 1983.
19. Nicoli, D., et. al., "Chemical Modification of Acrylamide Gels: Verification of the Role of Ionization in Phase Transitions," *Macromolecules*, Vol. 16, p. 887-891, 1983.
20. Osada, T. and Hasebe, M., "Electrically Actuated Mechanochemical Devices using Polyelectrolyte Gels," *Chemistry Letters*,", p. 1285-1288, 1985.
21. Suzuki, M., et. al., "An Artificial Muscle by Polyvinyl Alcohol Hydrogel Composites," *Proc. of IUPAC-CHEMRAWN VI*, Tokyo, 1987.
22. Tanaka, T., Soda, K. and Wada, A., "Dynamical Aspects of Helix-Coil Transitions in Biopolymers I," *Journal of Chemical Physics*, Vol. 58, p. 5707, 1973.
23. ———, Ishiwata, S and Ishimoto, C., "Critical Behavior of Density Fluctuations in Gels," *Physical Review Letters*, Vol. 38, p. 771, 1977.
24. ———, "Dynamics of Critical Concentration Fluctuations in Gels," *Physics Review*, V. A17, p. 763, 1978
25. ———, "Collapse of Gels and the Critical Endpoint," *Physical Review Letters*, Vol. 40, p. 820, 1978.
26. ——— and Fillmore, D. J., "Kinetics of Swelling of Gels," *Journal of Chemical Physics*, Vol. 70, p. 1214, 1979.
27. ———, "Phase Transition in Gels and a Single Polymer," *Polymer*, Vol. 20, p. 1404, 1979.

28. ———, et. al., “Phase Transition in Ionic Gels,” *Physical Review Letters*, Vol. 45, p. 1636, 1980.
29. ———, “Gels,” *Scientific American*, p. 124-138, January 1981.
30. ———, Nishio, I., Sun, S.T., and Ueno-Nishio, S., “Collapse of Gels under an Electric Field,” *Science*, Vol. 218, p. 467, 1982.
31. ———, et. al., “Mechanical instability of gels at the phase transition,” *Nature*, Vol. 325, No. 6107, pp. 796-798, February 26, 1987.
32. ———, “Gels,” in *Structure and Dynamics of Biopolymers*, edited by Nicolini, C., Martinus Nijhoff Publishers, Boston, p. 237-257, 1987.